Depolarization of Surface−Enhanced Fluorescence: An Approach to Fluorescence Polarization Assays

ARTICLE *in* ANALYTICAL CHEMISTRY · AUGUST 2008

Impact Factor: 5.64 · DOI: 10.1021/ac8003055 · Source: PubMed

2 AUTHORS:

Henryk Szmacinski
University of Maryland, Baltimore
155 PUBLICATIONS **4,002** CITATIONS

SEE PROFILE

Joseph R Lakowicz
University of Maryland Medical Center
878 PUBLICATIONS **42,262** CITATIONS

SEE PROFILE

Published in final edited form as:
Anal Chem. 2008 August 15; 80(16): 6260–6266. doi:10.1021/ac8003055.

Depolarization of Surface-Enhanced Fluorescence: An Approach to Fluorescence Polarization Assays

Henryk Szmacinski* and **Joseph R. Lakowicz**
Center for Fluorescence Spectroscopy, Department of Biochemistry and Molecular Biology, University of Maryland Baltimore, 725 West Lombard Street, Baltimore, Maryland 21201

Abstract

Localized surface plasmons of metallic particles of sub-wavelength sizes strongly modify the spectral properties of nearby fluorophores. The enhanced radiative decay rate leads to high fluorescence efficiencies and decreased fluorescence lifetimes. In this report we show that metal-enhanced fluorescence generated by the presence of the silver islands on the glass substrate displays high depolarization. Intensities, lifetimes, and emission anisotropies of several fluorophore protein conjugates have been studied in the absence and presence of metallic nanostructures. Despite highly decreased lifetimes of about 10-fold and immobilization of conjugates on the solid substrate, the observed emission anisotropies for all fluorophores on the metal-enhanced substrate decreased 300–500% compared to that in solution. This observation implies a new generation of fluorescence polarization immunoassays with broad applications because of no restrictions to the lifetime of the probe and the size of labeled biomolecules. The changes in polarization are due to binding that occur on the bioactive surface localized near the metal particles.

There is a growing interest in the optical properties of metallic nanostructures of subwavelength sizes that display localized surface plasmons that can be easily excited with incident electromagnetic waves and nearby excited fluorophores. Recently, several groups have begun using metallic nanostructures to generate fluorescence enhancements that have the potential for use in single molecule detection. The strong interaction between the free electrons in the metallic nanostructures and an incident electromagnetic field creates unique optical properties. Techniques to measure these properties include resonance light scattering (RLS),[1,2] distance-dependent scattering properties of nanoparticles,[3–5] or scattering and extinction properties of metal-dielectric nanoshells.[6,7] Coupling these metallic nanoparticles with fluorescent probes also resulted in unique effects based on near-field interactions. When fluorophores are within 3–50 nm from the surface of the metallic nanostructures, a plasmon–fluorophore interaction occurs providing a reduction in the fluorescence lifetime through an increased radiative decay rate while also enhancing the fluorescence intensity through an increased excitation field.[8–15] The effect has been called metal-enhanced (MEF) or surface-enhanced fluorescence (SEF). The result is improved photostability of brighter fluorophores due to a decrease in the time the fluorophore stays in the excited state. It has also been observed that the fluorophores under MEF conditions are less susceptible to optical saturation.[16] Theoretical calculations on surface enhanced fluorescence was also extensively published.[17–23] The phenomenon of fluorescence enhancement and decreased fluorescence lifetime are theoretically explained by modified radiative and nonradiative decay rates of fluorophores interacting with surface plasmons with strong dependence on distance between fluorophore and metal surface, transition moment orientation, wavelength, and quantum yield.

*Corresponding author. E-mail: henry@cfs.umbi.umd.edu. Fax: 410-706-8408.

Various configurations of single fluorophore relative to the particle surface have been studied. However, the reports on surface-enhanced fluorescence do not consider the level of emission polarization. Here we present experimental data on the anisotropy of surface-enhanced fluorescence. Our approach incorporates silver island films (SIFs) deposited on planar glass slides and several fluorophores conjugated to proteins that bind to the SIFs. The measurements included intensity, lifetime, and emission anisotropy for probes free in solution and when bound to the SIFs substrates. The observed effects imply a new generation of fluorescence polarization based sensing, in particular to immunoassays.

MATERIAL AND METHODS

Preparation of the Silver Island Films and Immobilization of Streptavidin Fluorophore Conjugates

Silver island films (SIFs) were deposited on quartz substrate. The wet chemical deposition method was used to coat the substrate with the SIFs. The procedure has been described elsewhere.[11,24] Briefly, the reduction of silver ions by D-glucose results in the deposition of the SIFs on the glass or quartz substrate. The absorption spectrum maximum of the SIFs is near 460 nm (optical density of about 1.25) which indicated that the particles were of subwavelength size. The wet chemical deposition technique results in a variability in the particle sizes and shapes as has been previously shown using atomic force microscopy with particle sizes up to 500 nm and thicknesses of 50–100 nm.[11] The fluorescence enhancement achieved via the silver islands strongly depends on the silver particle surface morphology where silver islands and silver colloids were deposited on the glass surface.[25] We used high density silver islands to limit the void areas between particles where the fluorophores would not effectively interact with particle plasmon resonance. The surface of SIFs was coated with biotinylated bovine serum albumin (BSA-bt). The BSA-bt was electrostatically immobilized on the SIFs through incubation in phosphate buffer at pH 7.4 for 1 h. After unbound BSA-bt was washed out, the streptavidin fluorophore conjugates were incubated for 1 h. A silicone adhesive with multiple wells, 2.0 mm in depth and 2.5 mm in diameter (Grace Bio-Laboratories), was placed on top of the substrate allowing for multiple samples to be investigated on the same substrate. For spectroscopic measurements, samples were kept in phosphate buffer.

Streptavidin dye conjugates Alexa Fluor 488-SA, Alexa Fluor 532-SA, Alexa Fluor 635-SA, and Alexa Fluor 680-SA were acquired from Invitrogen (Carlsbad, CA); DY495-SA and DY547-SA, from Pierce Biotechnology (Rockford, IL); Cy3-SA and Cy5-SA from GE Healthcare Life Sciences (Piscataway, NJ); and Fluorescein-4-Biotin (Fl-Bt) from Sigma Aldrich (St. Louis, MO). Buffer components and other chemicals were from Sigma-Aldrich.

Spectroscopic Measurements

The extinction spectrum of silver islands film was measured using a single beam spectrophotometer (Hewlett-Packard model 8543). The polarization scattering spectra of the SIFs were measured using the Varian fluorometer (Eclipse 4) in a synchronous mode, i.e., the excitation and emission monochromators were at the same wavelength.

Emission anisotropy measurements of probes in solution, bound to glass surface and bound to SIFs were performed using epi-illumination configuration (Figure 1). Light from LED was collimated with lens L1, polarized with a Glann–Thompson polarizer P1, and directed through excitation bandpass filter F1, dichroic spliter D, and lens L2 to the sample. The fluorescence emitted from the sample was collected with two orthogonal polarizations, one parallel and one perpendicular to the excitation polarization vector. The measured anisotropies were corrected for different detection sensitivities to two orthogonal polarizations using highly depolarized

emission of fluorescein-biotin in water with an anisotropy value of 0.026. The anisotropy value of fluorescein-biotin was determined using cuvette and L-format configuration with correction for the *G*-factor.[26] The epi-illumination alignment was also verified using a sample with Ludox, silica suspension in water, which is expected to result in polarization degree close to 1.0. It was found that the measured polarization of Ludox was about 0.94 which indicates that a high degree of polarization of excitation light has been achieved using LEDs and epi-illumination.

Fluorescence lifetimes were measured using frequency-domain (FD) fluorometer (K2 from ISS, Champaign, IL). The FD intensity decays were analyzed using the multiexponential model

$$I(t)=\sum_{i=1}^{n}\alpha_i \exp^{-t/\tau_i} \tag{1}$$

where τ_i are the decay times and α_i are the amplitudes and ($\Sigma_i\ \alpha_i = 1.0$). Amplitude weighted ($\langle\tau\rangle$) and mean lifetime (τ_M) were calculated

$$\langle\tau\rangle=\alpha_i\tau_i, \quad \tau_M=f_i\tau_i \tag{2}$$

where f_i are the fractional intensities and ($f_i = \alpha_i\tau_i\Sigma_i\ \alpha_i\tau_i$).

The excitation sources were light emitting diodes (LEDs) from Nichia (York, PA), blue LED (NSPB 500S) with maximum at 470 nm and red LED (Nichia NSPR633AS) with maximum at 633 nm. Because of the broad tails of LEDs that extend to long wavelengths, bandpass filters (F1, Figure 1) were used in the excitation path length. LEDs were modulated by applying an rf driving current to the LED in the frequency range from 5 to 350 MHz.[27,28] The blue LED was used for excitation of Fluorescein-Bt, Alexa Fluor 488, Alexa Fluor 532, DY495, DY547, and Cy 3 using the bandpass excitation filter 460/40 nm and the emission filter 555/50 (F1 and F2, respectively, Figure 1). The red LED was used for excitation of Alexa Fluor 635, Alexa Fluor 647, Alexa Fluor 680, and Cy 5 using an excitation bandpass filter 635/30 nm and a long pass emission filter above 667 nm.

RESULTS AND DISCUSSION

Spectral Characteristics of Dye–Streptavidin Conjugates in Solution

The spectroscopic properties of investigated dye–streptavidin conjugates in buffer solution are summarized in Table 1. The dye to protein ratio (D/P) varied from about 1.0 to 4.1. The spectral range of used dyes span a wide range of wavelengths from about 495 nm to about 685 nm. Intensity decays were fit to one- or two-exponential models, and the amplitude weighted and mean lifetimes were calculated. The calculated lifetimes illustrate the properties of various fluorophores, when used for labeling of proteins. The calculated amplitude weighted lifetimes are shorter then intensity weighted, especially if short lifetime components are present in intensity decays. This is well manifested for DY547-SA and Alexa Fluor 532-SA where the short components contribute significantly in the total emission, with fractional intensities of 0.8074 and 0.5032, respectively (Table 1). The origin of lifetime heterogeneity of fluorophores when conjugated to proteins can be due to various dye environments, hydrophobicity, as well as dye–dye interactions for high D/P ratios. Fluorophores with lifetimes shorter than about 2 ns usually are not considered for FPIAs. Therefore, the fluorescein is the most frequently used fluorophore for polarization assays because of its relatively long lifetime of about 4 ns resulting in low anisotropy of labeled small biomolecules.

Intensity and Lifetimes of Dye–Streptavidin Conjugates in the Presence of SIFs

The effect of the SIFs on fluorescence lifetimes and intensity enhancements are summarized in the Table 2. The fluorescence intensities are strongly enhanced in the presence of silver island films. The enhancement (*E*) factor varies from 6.8 for fluorescein-biotin to 14.2 for DY547-SA. The intensity enhancements were determined with comparison of samples prepared on SIFs relative to those on bare glass substrates. Intensity decays were fit to a two-exponential model resulting in a very short component of 40–210 ps with significant intensity contribution (more than 0.62 of fractional intensity) for most dyes. This short lifetime component is attributed to the strong fluorophores–plasmon interactions. The longer lifetime components are likely representative of the fluorophores that weakly interact with plasmons or fluorophores located on the glass between silver nanostructures. In our earlier studies of cyanine labeled DNA on SIFs, we also observed longer components with fractional intensities of about 0.2.[29] Frequency-domain intensity decays for fluorescein-biotin and for DY547-SA in solution and when bound to the SIFs surfaces are shown in Figure 2. There is observed a dramatic shift in frequency responses toward higher modulation frequencies because of the significant contribution of short lifetime components. Since we used LEDs for excitation, the modulation frequency range was limited to about 300 MHz and less lifetime resolution. It was shown that using a higher frequency range, up to 2 GHz, additional short components of less than 10 ps were resolved for Cy 3 and Cy 5 when bound to the SIFs.[29] Nonetheless, intensity decays measured here using simple excitation sources such as LEDs provide clear evidence on strong interaction of fluorophores with surface plasmons. It is observed that the amplitude weighted lifetime decreased approximately 10-fold for most fluorophores (see Table 1 and Table 2). The intensity-weighted lifetimes did not decrease as much because they are dominated by the long lifetime component.

Fluorescence Anisotropy

Fluorescence anisotropies of dye–streptavidin conjugates were first measured in the buffer solution. Because of the large molecular weight of streptavidin, the observed anisotropies are relatively high. The expected rotational correlation time of streptavidin in the buffer solution, which the size is similar to HSA (about 65 000 Da), is about 42 ns.[26] The observed fluorescence anisotropy values for dye–streptavidin conjugates in solution range from 0.087 to 0.203 (Table 3). Streptavidin–dye conjugates with high D/P ratios (Alexa Fluor 488-SA, Alexa Fluor 532-SA, and Alexa Fluor 647-SA) display lower anisotropies because of possible excitation energy transfer (homo-FRET) between multiple dyes which cause depolarization of the fluorescence.[30] Anisotropy values of streptavidin–dye conjugates were also measured when in the presence of excess of BSA-bt in solution and again when BSA-bt was fixed to a glass surface without SIFs. Binding of the streptavidin conjugates to the BSA-bt in solution or on the glass surface resulted in minor changes of anisotropy values (Table 3) indicating that the rotational correlation time of the streptavidin itself is sufficiently large compared to the lifetimes of the tested dyes.

In contrast to the conjugates in solution and bound to glass, the anisotropy values dramatically decreased when probes were bound to the SIF surface. This is a somewhat unexpected observation because one would expect, a priori, an increase in anisotropy due to the substantially reduced fluorescence lifetime and limited rotational motion upon binding to the SIFs compared to rotational motion allowed in solution. Surprisingly, while the lifetime of bound probes decreased several-fold and rotational motions were decreased upon binding to the SIFs, the fluorescence polarization decreased from 3- to 5-fold. The observed decreased polarizations were larger for fluorophores excited in the blue wavelength range than in the red. There are probably several reasons for the strong depolarization, which are discussed below.

One contribution may be related to the depolarized scatter which was observed from silver colloids.[31,32] It was shown that depolarization of incident light follows the extinction spectrum of silver colloids with polarization of up to 0.8 at the maximum of the extinction spectrum (optical density 0.16 and wavelength 425 nm for monodisperse silver colloids.[31]) For heterodisperse silver colloids, the anisotropy spectrum of the scattered light displayed more complex behavior and a larger degree of depolarization at longer wavelength (below 0.5).[32] The strongly depolarized light scattering from heterodisperse silver colloids has been recently modeled using interference of surface plasmon resonance modes occurring on the same metallic particles.[33] We measured the polarization spectrum along with the extinction spectrum of SIFs and found that the depolarization effect is less than 10% (Figure 3). The polarized incident light results in highly polarized scattered light indicating that the near-field evanescent field from silver island films is radiated into a far-field signal with highly preserved polarization over a broad range of wavelengths (polarization spectrum, Figure 3). This mean that highly depolarized emission in the presence of SIFs cannot be explained only by the depolarization effect of excitation light.

Additionally, with regard to emission, the fluorophores undergo near-field interactions with the metallic particles, which results in a more complex field distribution around the particle than is induced by far-field planar wave illumination. Hence, the emission will display a higher degree of depolarization than is observed from the polarization of the far-field scattered incident light. We believe that the random distribution of silver nanoparticles of various sizes and shapes in SIFs which display a broad wavelength band (see extinction spectrum in Figure 3) can support multimode surface plasmons that can be excited also by fluorophores in excited states, which is in agreement with recent theoretical calculations using the surface plasmon interference model.[33]

Therefore, the observed depolarization of emission can be due to strong interaction between excited fluorophores and particle plasmon resonance which leads to loss of the anisotropy observed from fluorophore alone. The multiple radiating systems consisting of excited fluorophores and silver particles radiate randomly as observed by depolarized far field signal. At first glance this result seems similar to the homotransfer between two identical fluorophores where energy migration always results in depolarization of emission.[30] Our sample of Alexa Fluor 488-SA is such an example where four fluorophores are attached to one streptavidin with already partially depolarized emission compared to very similar DY495-SA that has one fluorophore per streptavidin (Table 3). However, the analogy is not perfect because of the increased complexity of fluorophore–metal interactions.

The short lifetime accompanied with large intensity enhancement observed for each fluorophore when on the SIFs indicates that strong interaction between the excited fluorophores and the particle plasmon occurs. The local depolarization of the affected molecule due to SIFs is likely even higher than the observed composite values in the far field. This is because there is a fraction of fluorophores that do not interact (or interact weakly) with particle plasmon and thus increase the observed anisotropies. An estimation can be performed using additive properties of emission anisotropy[26]

$$r = f_1 r_1 + f_2 r_2 \tag{3}$$

where the r is observed anisotropy, the r_1 and r_2 are anisotropies associated with short and long lifetime component, respectively, and the f_1 and f_2 are fractional intensities of short and long lifetime components ($f_1 + f_2 = 1$), respectively. Using the values in Table 2, one can estimate that the contribution of the long lifetime component accounts approximately for 40–60% of the measured anisotropies on the SIFs. For example, for Alexa Fluor 532, the fractional

intensity of the long component, f_1 = 0.1451 (Table 2), which multiplied by r_1 = 0.094 (anisotropy on glass, Table 3) results in 0.014, which is 40% of the measured value of 0.035.

Potential for Plasmon Polarization Assays

The observed depolarized MEF-P emissions have promising advantages for design of polarization based affinity assays, such as immunoassays, and studies of interactions between biomolecules. Traditionally, the FPIAs relied on labeling relatively small biomolecule (usually less than 10 kDa) with fluorophores that display relatively long lifetime (usually Fluorescein with about 4 ns) to obtain depolarized fluorescence from the unbound probe. The FPIAs relies on the increase of the emission anisotropy when probe binds to large target molecules due to the change of rotational correlation time. Fluorescence anisotropy is inversely proportional to the rate of fluorophore rotational correlation time in solution

$$r=\frac{r_0}{1+\frac{\tau}{\tau_C}} \tag{4}$$

where τ is the lifetime of the excited-state and τ_C is the rotational correlation time (the time for anisotropy to decrease 1/e of its limiting value and r_0, which is a photophysical constant which depends upon the probe used). For globular proteins, the rotational correlation time is related to the molecular weight of the molecule (MW) as follows26

$$\tau_C=\frac{\eta \mathrm{MW}}{RT}(v+h) \tag{5}$$

where η is the solution viscosity in poise, MW the molecular weight of the probe or complex, R the universal gas constant, T is the temperature in K, v is the specific volume of the protein, typically near 0.73 cm^3/g, and h is the hydration, near 0.23 g of H_2O per gram of protein. Thus, traditional FPIAs performed with organic dyes that display lifetimes in the nanosecond range require low molecular weight molecules for labeling. As one can see, then none of the dye–streptavidin conjugates can be regarded as conventional polarization probes because they do not display a useful change in anisotropy values when bound to the biotinylated BSA in solution (Table 3). This is because the molecular weight of streptavidin of about 66 kDa results in a rotational correlation time of about 26 ns in aqueous solution that can be estimated from eq 3 (viscosity of about 1 cP at 25 °C). The observed rotational correlation times for many proteins are usually about 2-fold larger than calculated because of the nonspherical shapes and larger effective solvent shell for rotational diffusion than for hydration.26

In contrast, all dye–streptavidin conjugates can be regarded as excellent polarization probes for detection of biotinylated proteins when binding occurs on the surface with metal nanoparticles, which supports fluorophore–plasmon interaction. This is because the mechanism for depolarization is not due to change in molecular weight due to binding (or dissociation) but the localized space where the bimolecular interaction occurs.

Simple simulations are used here to show that a fluorophore labeled large biomolecule can be used for the design of MEF-P assays where the binding will occur on the surface of the MEF substrate. The binding event places the fluorophore in proximity to metallic particles where the fluorophore–plasmon interaction cause depolarization of the fluorescence emission. Equations 4 and 5 for rotating molecules do not apply to MEF-P assays where the detection molecule is bound to the functionalized substrate. Figure 4 shows simulated results of the MEF-

P assay, where the free detection probe displays an anisotropy of 0.2 and when bound to the target molecule on the MEF substrate, the emission is depolarized to an anisotropy value of 0.02 and the intensity is enhanced 10-fold. Because of the increased intensity upon binding, the MEF-P method will result in more sensitive assays because a small number of bound detection molecules will contribute significantly in the total emission.

For comparison, a typical polarization assay is also shown where the free probe displays a low anisotropy of 0.02 and when bound to a large molecule the anisotropy increases to 0.2 without a change in the intensity upon binding (Figure 4). Assuming that fractional intensities are proportional to the number of respective molecules, one can rewrite eq 3 and express the relation between the molar ratio of bound to free probes (N_B/N_F) with the observed anisotropy (r)

$$\frac{N_B}{N_F}=\frac{r-r_F}{r_B-r}\frac{1}{E} \tag{6}$$

where the r_F and r_B are the anisotropies of free and bound probes, respectively, and the E is the intensity enhancement of the probe upon binding. In the standard FPIAs, the factor E is usually close to 1.0 (probe does not change intensity upon binding); however, in the case of MEF, the E factor is much larger than 1.0 (see Table 2).

The measurement and analysis of data are the same for MEF-P as for the standard polarization assay. One can rewrite eq 6 and express the fraction of bound fluorescently labeled molecules as a function of measured anisotropy[26,34] r

$$F_B=\frac{r-r_F}{(r_B-r)E+(r-r_F)} \tag{7}$$

For the standard polarization assay, the factor E represents the intensity ratio of bound to free form of the probe.[26,34] Equation 7 is simply related to the traditional binding assays and represents the ratio of complex to the total labeled receptor concentration.[34]

Because the change in polarization of metal enhanced fluorescence (MEF-P) is not due to changes in molecular volume of the bound complex, there are several advantages of MEF-P for future applications to molecular sensing. (1) Because most fluorophores interact with metal particles, the MEF-P assay can be performed with any fluorophore. The suitability of MEF-P is not limited by the lifetime of the dye. (2) Large biomolecules can be labeled with fluorophores because the changes in polarization are due to the binding event and not to a change in rotational diffusion. The labeled molecules can be large antibodies that bind to small unlabeled antigens. The large change in molecular volume is not required for MEF-P assays. (3) The sensitivity of MEF-P will be better than traditional FP assays because the bound probe displays enhanced intensity compared to that of the unbound. This means that a small fraction of bound probes will generate large changes in anisotropy. Figure 4 shows that the detection of a lower concentration of bound probes will be possible using the MEF-P assay compared to the conventional FPIA. To the first approximation, detection of the bound probe will be improved proportionally to the enhanced intensity of the bound probes (here 10-fold). (4) High signal-to-noise ratio in polarization measurements will be obtained because of a large change in anisotropy which affords a large dynamic range. In standard FPIA, the useful anisotropy change is from the anisotropy value of the free probe to that of the complex. The value of anisotropy of the free probe strongly depends on the molecular weight of the labeled biomolecule which

usually decreases the useful change in anisotropy between the free probe and the complex. In the MEF-P approach, the anisotropy of the complex will be always low regardless of the molecular weight of interacting biomolecules, thus the anisotropy change is expected to be large (determined by the value of labeled free probe).

These advantages will substantially broaden and increase sensitivity of the FPIA applications. The typical calibration curve for conventional FPIA needs a low anisotropy probe which is restricted to fluorescein and low MW biomolecules. In contrast, the MEF-P based assay requires a large anisotropy probe which can be easy obtained because of the choice of many fluorophores and labeling moderate or large MW biomolecules. For example, studies of binding between cellular receptor CD4 (~40 kDa) and the HIV-1 viral envelope glycoprotein gp120 (~100 kDa) has been performed using polarization assays where a small peptide CD4M33 (about 3 kDa) was synthesized and labeled with fluorescein to mimic the interaction between CD4 and gp120.[35] One can foresee that MEF-P approach will allow direct labeling of CD4 or gp120 without the requirement for a small tracer and study their bindings in the presence of various inhibitors. The complex on the MEF substrate will exhibit highly depolarized emission due to plasmon–fluorophore interaction compared to high polarization of the free probe (large molecular weight). The sensitivity of MEF-P based assays are expected to be significantly improved because of enhanced emission of bound probes. In addition, the MEF-P assays will require very small quantities of biochemicals because the receptor concentration is defined by surface density to which labeled ligand will bind (or dissociate).

CONCLUSIONS

In this report, the depolarization of metal-enhanced fluorescence was demonstrated. While the lifetime of bound probes decreased several-fold and rotational motions were decreased upon binding to the SIFs, the fluorescence polarization decreased from 3 to 5-fold. The observed decreased polarizations were larger for fluorophores excited in the blue wavelength range than in the red. The observed depolarized metal enhanced emission has promising advantages for design polarization based immunoassays and studies of interactions between biomolecules with direct labeling of large biomolecules.

Acknowledgments

This work was supported by the NIH Grants NIBIB EB006521 and NHGRI HG 002655.

References

1. Fang B, Gao Y, Li M, Wang G, Li Y. Microchim Acta 2004;147:81–86.
2. Wang Z, Lee J, Cossins AR, Brust M. Anal Chem 2005;77:5770–5774. [PubMed: 16131095]
3. Storhoff JJ, Lucas AD, Garimella V, Bao YP, Muller UR. Nat Biotechnol 2004;22:883–887. [PubMed: 15170215]
4. Elghanian R, Storhoff JJ, Mucic RC, Letsinger RL, Mirkin CA. Science 1997;277:1078–1081. [PubMed: 9262471]
5. Nam JM, Thaxton CS, Mirkin CA. Science 2003;301:1884–1886. [PubMed: 14512622]
6. Kumar S, Harrison N, Richards-Kortum R, Sokolov K. Nano Lett 2007;7(5):1338–1343. [PubMed: 17439187]
7. Hirsh LR, Jackson JB, Lee A, Halas NJ, West JL. Anal Chem 2003;75:2377–2381. [PubMed: 12918980]
8. Weitz DA, Garoff S, Gersten JI, Nitzan A. J Chem Phys 1983;78(9):5324–5338.
9. Kummerlen J, Leitner A, Brunner H, Aussenegg FR, Wokaun A. Mol Phys 1993;80(5):1031–1046.
10. Sokolov K, Chumanov G, Cotton T. Anal Chem 1998;70:3898–3905. [PubMed: 9751028]

11. Lakowicz JR, Shen Y, Dauria S, Malicka J, Fang J, Gryczynski Z, Gryczynski I. Anal Biochem 2002;301:261–277. [PubMed: 11814297]
12. Maliwal BP, Malicka J, Gryczynski Z, Gryczynski I, Lakowicz JR. Biopolymers (Biospectroscopy) 2003;70:585–594. [PubMed: 14648768]
13. Malicka J, Gryczynski I, Gryczynski Z, Lakowicz JR. Anal Biochem 2003;315:57–66. [PubMed: 12672412]
14. Matveeva EG, Gryczynski I, Barnett A, Leonenko Z, Lakowicz JR, Gryczynski Z. Anal Biochem 2007;361:239–245. [PubMed: 17316540]
15. Gerber S, Reil F, Hohenester U, Chlagenhaufen T, Krenn JR, Leitner A. Phys Rev B 2007;75:073404.
16. Malicka J, Gryczynski I, Fang J, Kusba J, Lakowicz JR. J Fluoresc 2002;12:435–446.
17. Gersten J, Nitzan A. J Chem Phys 1981;75(3):1139–1152.
18. Garoff S, Weitz DA, Alvarez MS, Gersten JI. J Chem Phys 1984;81(11):5189–5200.
19. Das P, Metiu H. J Phys Chem 1985;89:4680–4687.
20. Guzatov DV, Klimov VV. Chem Phys Lett 2005;412:341–346.
21. Bharadwaj P, Novotny L. Opt Express 2007;15(12):14266. [PubMed: 19550702]
22. Blanco LA, Garcia de Abajo FJ. Phys Rev B 2004;69:205414.
23. Mertens H, Koenderink AF, Polman A. Phys Rev B 2007;76:115123.
24. Ni F, Cotton M. Anal Chem 1986;58:3159–3163. [PubMed: 3813029]
25. Lukomska J, Malicka J, Gryczynski I, Lakowicz JR. J Fluoresc 2004;14(4):417–423. [PubMed: 15617384]
26. Lakowicz, JR. Principles of Fluorescence Spectroscopy. Vol. 3. Springer Science; New York: 2006. p. 353-382.
27. Sipior J, Carter GM, Lakowicz JR, Rao G. Rev Sci Instrum 1996;67(11):3795–3798.
28. Szmacinski H, Chang Q. Appl Spectrosc 2000;54:106–109.
29. Malicka J, Gryczynski I, Fang J, Lakowicz JR. Anal Biochem 2003;317:136–146. [PubMed: 12758251]
30. Kawski A. Crit Rev Anal Chem 1993;23:459–529.
31. Gryczynski Z, Lukomska J, Lakowicz JR, Matveeva EG, Gryczynski I. Chem Phys Lett 2006;421:189–192.
32. Klitgaard S, Shtoyko T, Calander N, Gryczynski I, Matveeva EG, Borejdo J, Neves-Petersen MT, Petersen SB, Gryczynski Z. Chem Phys Lett 2007;443:1–5.
33. Calander N, Gryczynski I, Gryczynski Z. Chem Phys Lett 2007;434:326–330. [PubMed: 18516244]
34. Lundblad JR, Laurance M, Goodman RH. Mol Endocrinol 1996;10:607–612. [PubMed: 8776720]
35. Stricher F, Martin L, Barthe P, Pogenberg V, Mechulam A, Menez A, Roumestand C, Veas F, Royer C, Vita C. Biochem J 2005;390:29–39. [PubMed: 15836438]

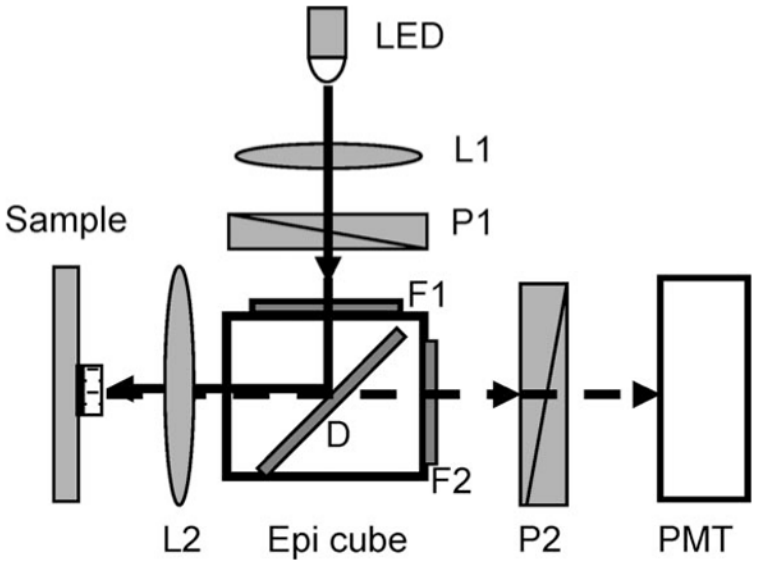

Figure 1.
Scheme of experimental configuration for emission anisotropy measurements. The excitation pathway is shown in solid and emission in dashed arrows.

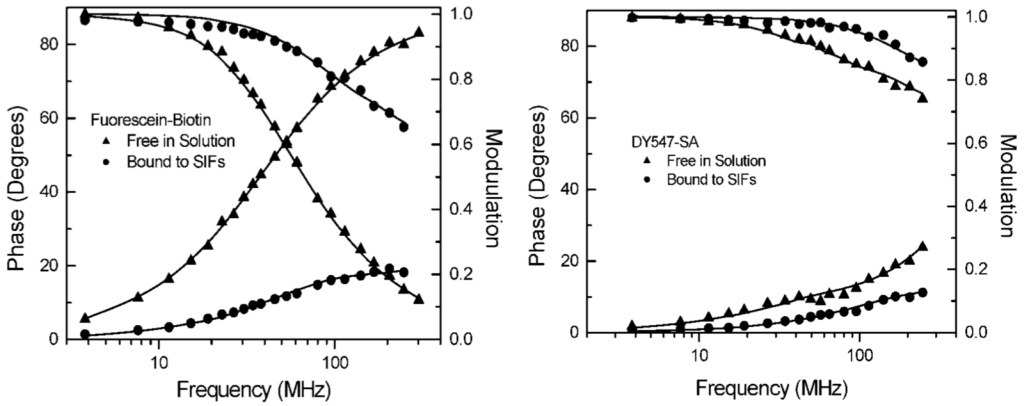

Figure 2.
Intensity decays of the fluorescein-biotin (left) and DY547-SA (right) when free in solution and bound to the SIFs.

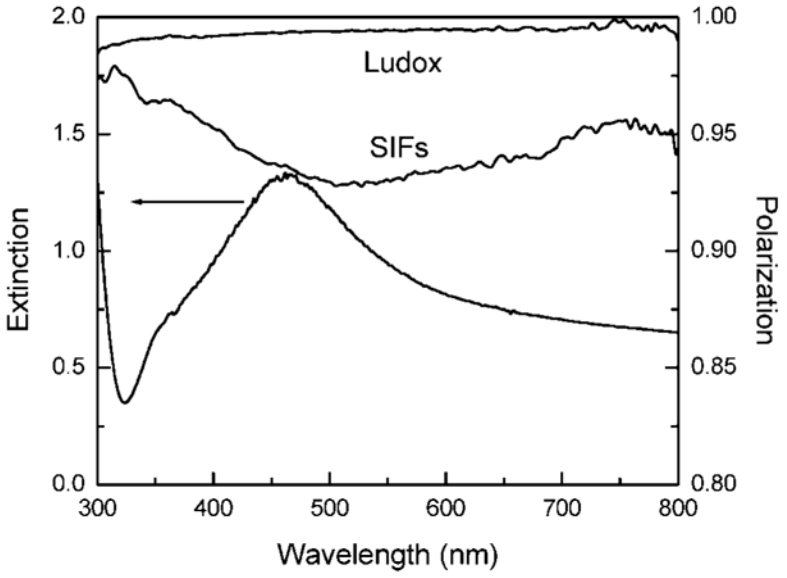

Figure 3.
Extinction and polarization spectra of SIFs on a glass substrate. The polarization spectrum of silica particle suspension (Ludox) is shown for comparison.

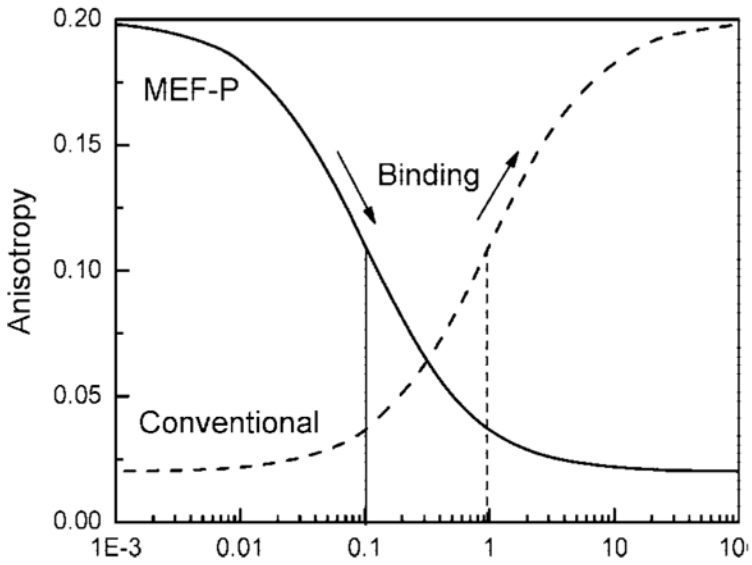

Figure 4.
A comparison of the simulated data for MEF-P (solid line) with conventional FPIA (dashed line) according eq 5. The arrows show the change in anisotropies upon binding, and the vertical lines indicate the mid points.

Table 1

Spectral Properties of Protein Conjugated Dyes in Solution[a]

				intensity decays				
dye	**D/P**	ε	$\lambda_{ABS}/\lambda_{EMS}$	τ_i (ns)	α_i	f_i	$\langle\tau\rangle$	τ_M
Fluorescein-Bt	N/A	68 000	494/518	4.11	1.0	1.0	4.11	4.11
AlexaFluor 488	3.9	71 000	495/519	3.08	0.4778	0.7382	1.759	2.418
				0.55	0.5222	0.2618		
DY495	1.0	70 000	495/520	3.91	0.4519	0.7991	2.211	3.287
				0.81	0.5481	0.2009		
AlexaFluor 532	4.1	81 000	529/551	2.60	0.1530	0.4968	0.804	1.533
				0.48	0.8470	0.5032		
DY547	1.0	150 000	553/572	3.76	0.0159	0.1926	0.316	0.934
				0.26	0.9841	0.8074		
Cy 3	1.7	150 000	558/578	1.23	0.3145	0.6684	0.579	0.915
				0.28	0.6855	0.3316		
AlexaFluor 635	1.5	140 000	632/647	4.88	0.3977	0.4681	3.995	4.037
				3.41	0.6023	0.5139		
AlexaFluor 647	2.7	239 000	653/669	2.11	0.6260	0.4447	1.485	1.183
				0.44	0.3740	0.5553		
Cy 5	0.9	250 000	657/678	1.86	1.0	1.0	1.86	1.86
AlexaFluor 680	2.8	184 000	679/685	1.98	1.0	1.0	1.98	1.98

[a] Dye-to protein ratio (D/P), extinction coefficient (ε) in (M^{-1} cm^{-1}), wavelength at maximum of absorption and emission spectra ($\lambda EXC/\lambda EMS$), and intensity decays (τ_i, lifetimes are in nanoseconds).

Table 2

Intensity Enhancement (*E*) and Intensity Decays of Various Dye–Streptavidin Conjugates Immobilized to the SIFs through the BSA-bt Spacer

dye	*E*	τ_i (ns)	α_i	f_i	$\langle\tau\rangle$	τ_m
Fluorescein[a]	**6.8**	**2.0**	**0.0335**	**0.3762**	**0.182**	**0.827**
		0.12	0.9665	0.6238		
AlexaFluor 488	7.5	1.28	0.0361	0.2496	0.181	0.424
		0.14	0.9639	0.7504		
DY495	9.1	1.76	0.0336	0.3698	0.157	0.714
		0.10	0.9664	0.6302		
AlexaFluor 532	11.2	2.25	0.0096	0.1451	0.140	0.429
		0.12	0.9914	0.8549		
DY547	14.2	0.87	0.0155	0.2355	0.052	0.235
		0.04	0.9845	0.7645		
Cy 3	9.8	2.06	0.0106	0.1763	0.120	0.446
		0.10	0.9804	0.8237		
AlexaFluor 635	12.4	2.19	0.0378	0.3259	0.256	0.835
		0.18	0.9622	0.6741		
AlexaFluor 647	8.1	1.19	0.0486	0.2593	0.220	0.434
		0.17	0.9514	0.7407		
Cy 5	9.0	2.02	0.0333	0.3034	0.222	0.724
		0.16	0.9667	0.6966		
AlexaFluor 680	14.1	2.02	0.0318	0.2736	0.267	0.705
		0.21	0.9682	0.7264		

[a]Fluorescein-biotin was attached to SIFs via layers of BSA-bt and avidin.

Table 3

Emission Anisotropies of Streptavidin Conjugated Fluorophores Free and Bound to BSA-bt in Various Environments[a]

dye	free	bound to BSA-bt	bound to BSA-bt on glass	bound to BSA-bt on SIFs
Fluorescein-Bt	0.021	0.194[b]	0.191[c]	0.038[c]
AlexaFluor 488	0.087	0.088	0.087	0.036
DY495	0.129	0.150	0.127	0.035
AlexaFluor 532	0.139	0.128	0.094	0.035
DY547	0.203	0.202	0.109	0.034
Cy 3	0.146	0.137	0.112	0.037
AlexaFluor 635	0.143	0.148	0.067	0.062
AlexaFluor 647	0.087	0.094	0.069	0.061
Cy 5	0.134	0.160	0.098	0.057
AlexaFluor 680	0.125	0.174	0.106	0.042

[a] The samples were kept in buffer solution.

[b] Fluorescein-biotin was saturated in buffer solution with avidin.

[c] Fluorescein-biotin was bound to the glass and SIFs surfaces via BSA-bt-avidin layers.